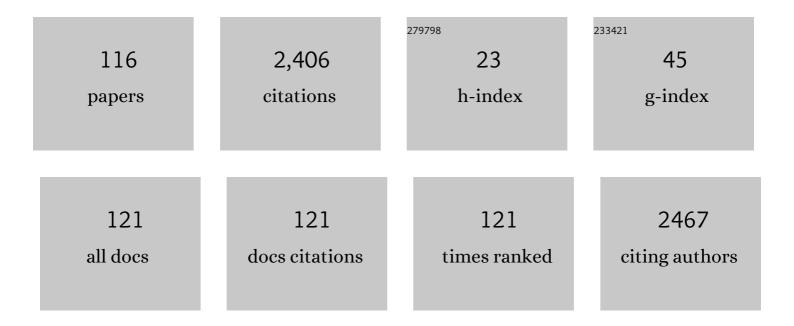
## Maria F Santarelli

List of Publications by Year in descending order

Source: https://exaly.com/author-pdf/1596602/publications.pdf Version: 2024-02-01



#	Article	IF	CITATIONS
1	Multislice multiecho T2* cardiovascular magnetic resonance for detection of the heterogeneous distribution of myocardial iron overload. Journal of Magnetic Resonance Imaging, 2006, 23, 662-668.	3.4	173
2	Beyond amygdala: Default Mode Network activity differs between patients with Social Phobia and healthy controls. Brain Research Bulletin, 2009, 79, 409-413.	3.0	165
3	An accurate and robust method for unsupervised assessment of abdominal fat by MRI. Journal of Magnetic Resonance Imaging, 2004, 20, 684-689.	3.4	140
4	Independent component analysis applied to the removal of motion artifacts from electrocardiographic signals. Medical and Biological Engineering and Computing, 2008, 46, 251-261.	2.8	134
5	StandardizedT2* map of normal human heartin vivo to correctT2* segmental artefacts. NMR in Biomedicine, 2007, 20, 578-590.	2.8	119
6	Improved T2* assessment in liver iron overload by magnetic resonance imaging. Magnetic Resonance Imaging, 2009, 27, 188-197.	1.8	119
7	Accurate segmentation of subcutaneous and intermuscular adipose tissue from MR images of the thigh. Journal of Magnetic Resonance Imaging, 2009, 29, 677-684.	3.4	79
8	Automated cardiac MR image segmentation: theory and measurement evaluation. Medical Engineering and Physics, 2003, 25, 149-159.	1.7	75
9	Evaluation of a web-based network for reproducible T2* MRI assessment of iron overload in thalassemia. International Journal of Medical Informatics, 2009, 78, 503-512.	3.3	71
10	A Fast and Effective Method to Assess Myocardial Necrosis by Means of Contrast Magnetic Resonance Imaging. Journal of Cardiovascular Magnetic Resonance, 2005, 7, 487-494.	3.3	67
11	A fast and accurate simulator for the design of birdcage coils in MRI. Magnetic Resonance Materials in Physics, Biology, and Medicine, 2002, 15, 36-44.	2.0	64
12	Preferential patterns of myocardial iron overload by multislice multiecho <i>T</i> * <sub>2</sub> CMR in thalassemia major patients. Magnetic Resonance in Medicine, 2010, 64, 211-219.	3.0	64
13	[18F]-Florbetaben PET/CT for Differential Diagnosis Among Cardiac Immunoglobulin Light Chain, Transthyretin Amyloidosis, andÂMimicking Conditions. JACC: Cardiovascular Imaging, 2021, 14, 246-255.	5.3	51
14	Realâ€ŧime cardiac metabolism assessed with hyperpolarized [1â€ <sup>13</sup> C]acetate in a largeâ€animal model. Contrast Media and Molecular Imaging, 2015, 10, 194-202.	0.8	44
15	Multislice multiecho T2* cardiac magnetic resonance for the detection of heterogeneous myocardial iron distribution in thalassaemia patients. NMR in Biomedicine, 2009, 22, 707-715.	2.8	42
16	Conductor geometry and capacitor quality for performance optimization of low-frequency birdcage coils. Concepts in Magnetic Resonance, 2004, 20B, 9-16.	1.3	41
17	Assessment of realâ€time myocardial uptake and enzymatic conversion of hyperpolarized [1â€ <sup>13</sup> C]pyruvate in pigs using slice selective magnetic resonance spectroscopy. Contrast Media and Molecular Imaging, 2012, 7, 85-94.	0.8	40
18	Magnetostatic simulation for accurate design of low field MRI phased-array coils. Concepts in Magnetic Resonance Part B, 2007, 31B, 140-146.	0.7	35

#	Article	IF	CITATIONS
19	Sensing Glove for Brain Studies: Design and Assessment of Its Compatibility for fMRI With a Robust Test. IEEE/ASME Transactions on Mechatronics, 2008, 13, 345-354.	5.8	35
20	Low-Field MR Coils: Comparison between Strip and Wire Conductors. Applied Magnetic Resonance, 2010, 39, 391-399.	1.2	31
21	Automatic correction of intensity inhomogeneities improves unsupervised assessment of abdominal fat by MRI. Journal of Magnetic Resonance Imaging, 2008, 28, 403-410.	3.4	29
22	Influence of myocardial fibrosis and blood oxygenation on heart T2* values in thalassemia patients. Journal of Magnetic Resonance Imaging, 2009, 29, 832-837.	3.4	28
23	Hyperpolarized MRS surface coil: Design and signalâ€ŧoâ€noise ratio estimation. Medical Physics, 2010, 37, 5361-5369.	3.0	24
24	Noise correlations and SNR in phased-array MRS. NMR in Biomedicine, 2010, 23, 66-73.	2.8	23
25	Multichannel Techniques for Motion Artifacts Removal from Electrocardiographic Signals. , 2006, 2006, 3391-4.		22
26	Numerical Calculation of Peak-to-Average Specific Absorption Rate on Different Human Thorax Models for Magnetic Resonance Safety Considerations. Applied Magnetic Resonance, 2010, 38, 337-348.	1.2	21
27	A novel tool for estimation of magnetic resonance occupational exposure to spatially varying magnetic fields. Magnetic Resonance Materials in Physics, Biology, and Medicine, 2011, 24, 323-330.	2.0	21
28	Coil sensitivity map-based filter for phased-array image reconstruction in Magnetic Resonance Imaging. International Journal of Biomedical Engineering and Technology, 2007, 1, 4.	0.2	20
29	Standardized T2* Map of a Normal Human Heart to Correct T2* Segmental Artefacts; Myocardial Iron Overload and Fibrosis in Thalassemia IntermediaVersusThalassemia Major Patients and Electrocardiogram Changes in Thalassemia Major Patients. Hemoglobin, 2008, 32, 97-107.	0.8	20
30	Classical and lateral skin effect contributions estimation in strip MR coils. Concepts in Magnetic Resonance Part B, 2012, 41B, 57-61.	0.7	20
31	B1+/actual flip angle and reception sensitivity mapping methods: simulation and comparison. Magnetic Resonance Imaging, 2011, 29, 717-722.	1.8	19
32	Fast generation of T2⎠maps in the entire range of clinical interest: Application to thalassemia major patients. Computers in Biology and Medicine, 2015, 56, 200-210.	7.0	19
33	Hyperpolarized 13C MRS Cardiac Metabolism Studies in Pigs: Comparison Between Surface and Volume Radiofrequency Coils. Applied Magnetic Resonance, 2012, 42, 413-428.	1.2	18
34	How the signalâ€ŧoâ€noise ratio influences hyperpolarized <sup>13</sup> C dynamic MRS data fitting and parameter estimation. NMR in Biomedicine, 2012, 25, 925-934.	2.8	18
35	A model of ultrasound backscatter for the assessment of myocardial tissue structure and architecture. IEEE Transactions on Biomedical Engineering, 1996, 43, 901-911.	4.2	17
36	Deep-learning-based cardiac amyloidosis classification from early acquired pet images. International Journal of Cardiovascular Imaging, 2021, 37, 2327-2335.	1.5	16

#	Article	IF	CITATIONS
37	A real-time adaptive filtering approach to motion artefacts removal from ECG signals. International Journal of Biomedical Engineering and Technology, 2010, 3, 233.	0.2	15
38	Automatic 2D registration of renal perfusion image sequences by mutual information and adaptive prediction. Magnetic Resonance Materials in Physics, Biology, and Medicine, 2013, 26, 325-335.	2.0	15
39	3D CMR Mapping of Metabolism by Hyperpolarized 13C-Pyruvate in Ischemia–Reperfusion. JACC: Cardiovascular Imaging, 2013, 6, 743-744.	5.3	15
40	Computational Analysis of a Radiofrequency Knee Coil for Low-Field MRI Using FDTD. Applied Magnetic Resonance, 2013, 44, 389-400.	1.2	14
41	Real-time multimodal medical image processing: a dynamic volume-rendering application. IEEE Transactions on Information Technology in Biomedicine, 1997, 1, 171-178.	3.2	13
42	Molecular Imaging: Its Application In Cardiovascular Diagnosis. Current Pharmaceutical Design, 2005, 11, 2225-2234.	1.9	12
43	Frequency domain approach to blind source separation in ECG monitoring by wearable system. , 2005, , .		12
44	Sample-Induced Resistance Estimation in Magnetic Resonance Experiments: Simulation and Comparison of Two Methods. Applied Magnetic Resonance, 2011, 40, 351-361.	1.2	12
45	DNP Methods for Cardiac Metabolic Imaging with Hyperpolarized [1-13C]pyruvate Large Dose Injection in Pigs. Applied Magnetic Resonance, 2012, 43, 299-310.	1.2	12
46	A fast and accurate simulator for the design of birdcage coils in MRI. Magnetic Resonance Materials in Physics, Biology, and Medicine, 2002, 15, 36-44.	2.0	11
47	A new method for quantitative cellular imaging on 3-D scaffolds using fluorescence microscopy. IEEE Transactions on Nanobioscience, 2003, 2, 110-117.	3.3	11
48	A Conway–Maxwell–Poisson (CMP) model to address data dispersion on positron emission tomography. Computers in Biology and Medicine, 2016, 77, 90-101.	7.0	11
49	A quadrature lowpass birdcage coil for a vertical low field MRI scanner. Concepts in Magnetic Resonance, 2004, 22B, 1-6.	1.3	10
50	Ultrasound Techniques for Drug Delivery in Cardiovascular Medicine. Current Drug Discovery Technologies, 2008, 5, 328-332.	1.2	10
51	Coil Sensitivity Estimation with Perturbing Sphere Method: Application to 13C Birdcages. Applied Magnetic Resonance, 2012, 42, 511-518.	1.2	10
52	Fundamentals in Cardiovascular Imaging Technologies. Current Pharmaceutical Design, 2008, 14, 1745-1752.	1.9	9
53	Magnetic resonance butterfly coils: Design and application for hyperpolarized 13C studies. Measurement: Journal of the International Measurement Confederation, 2013, 46, 3282-3290.	5.0	9
54	Design of a quadrature surface coil for hyperpolarized <sup>13</sup> C MRS cardiac metabolism studies in pigs. Concepts in Magnetic Resonance Part B, 2013, 43, 69-77.	0.7	9

#	Article	IF	CITATIONS
55	Estimation of occupational exposure to static magnetic fields due to usual movements in magnetic resonance units. Concepts in Magnetic Resonance Part B, 2014, 44, 75-81.	0.7	9
56	Variable density randomized stack of spirals (VDRâ€Ⓢ) for compressive sensing MRI. Magnetic Resonance in Medicine, 2016, 76, 59-69.	3.0	9
57	Estimation of pancreatic R2* for iron overload assessment in the presence of fat: a comparison of different approaches. Magnetic Resonance Materials in Physics, Biology, and Medicine, 2018, 31, 757-769.	2.0	9
58	Cardiac amyloidosis detection by early bisphosphonate (99mTc-HMDP) scintigraphy. Journal of Nuclear Cardiology, 2022, 29, 307-318.	2.1	9
59	Cardiac amyloidosis characterization by kinetic model fitting on [18F]florbetaben PET images. Journal of Nuclear Cardiology, 2022, 29, 1919-1932.	2.1	9
60	The Core of Medical Imaging: State of the Art and Perspectives on the Detectors. Electronics (Switzerland), 2021, 10, 1642.	3.1	9
61	Automatic Characterization of Myocardial Perfusion in Contrast Enhanced MRI. Eurasip Journal on Advances in Signal Processing, 2003, 2003, 1.	1.7	8
62	Experimental approaches to cardiac imaging with hyperpolarized [1-13c]pyruvate: a feasibility study in rats with a 3T clincal scanner. Journal of Cardiovascular Magnetic Resonance, 2010, 12, .	3.3	8
63	FDTD Analysis of a Radiofrequency Knee Coil for Low-Field MRI: Sample-Induced Resistance and Decoupling Evaluation. Applied Magnetic Resonance, 2013, 44, 1393-1403.	1.2	8
64	Improving sodium Magnetic Resonance in humans by design of a dedicated 23Na surface coil. Measurement: Journal of the International Measurement Confederation, 2014, 50, 285-292.	5.0	8
65	Non-compact myocardium assessment by cardiac magnetic resonance: dependence on image analysis method. International Journal of Cardiovascular Imaging, 2018, 34, 1227-1238.	1.5	8
66	New Technological Developments in the Clinical Imaging of Atherosclerotic Plaque. Current Pharmaceutical Design, 2003, 9, 2403-2415.	1.9	8
67	Myocardial perfusion by first pass contrast magnetic resonance: a robust method for quantitative regional assessment of perfusion reserve index. Heart, 2006, 92, 689-690.	2.9	7
68	Cardiac metabolism with hyperpolarized [1-13c]pyruvate: a feasibility study in mini-pig with a large dose injection. Journal of Cardiovascular Magnetic Resonance, 2010, 12, .	3.3	7
69	Cardiac Metabolism in a Pig Model of Ischemia–Reperfusion by Cardiac Magnetic Resonance with Hyperpolarized 13C-Pyruvate. IJC Metabolic & Endocrine, 2015, 6, 17-23.	0.5	7
70	Biomolecular imaging of 13C-butyrate with dissolution-DNP: Polarization enhancement and formulation for in vivo studies. Spectrochimica Acta - Part A: Molecular and Biomolecular Spectroscopy, 2018, 199, 153-160.	3.9	7
71	Non-linear prediction for oesophageal voice analysis. Medical Engineering and Physics, 2002, 24, 529-533.	1.7	6
72	A Robust Method for Assessment of Iron Overload in Liver by Magnetic Resonance Imaging. Annual International Conference of the IEEE Engineering in Medicine and Biology Society, 2007, 2007, 2895-8.	0.5	6

#	Article	IF	CITATIONS
73	Accelerated PET kinetic maps estimation by analytic fitting method. Computers in Biology and Medicine, 2018, 99, 221-235.	7.0	6
74	Imaging Techniques as an Aid in the Early Detection of Cardiac Amyloidosis. Current Pharmaceutical Design, 2021, 27, 1878-1889.	1.9	6
75	Deep Learning Staging of Liver Iron Content From Multiecho MR Images. Journal of Magnetic Resonance Imaging, 2023, 57, 472-484.	3.4	6
76	3D Medical Image Processing. , 2008, , 67-85.		5
77	The Biological Effects of Diagnostic Cardiac Imaging. Current Pharmaceutical Design, 2009, 15, 1123-1130.	1.9	5
78	Transmit-Only/Receive-Only Radiofrequency System for Hyperpolarized 13C MRS Cardiac Metabolism Studies in Pigs. Applied Magnetic Resonance, 2013, 44, 1125-1138.	1.2	5
79	Efficiency evaluation of a 13C Magnetic Resonance birdcage coil: Theory and comparison of four methods. Measurement: Journal of the International Measurement Confederation, 2013, 46, 2201-2205.	5.0	5
80	Technological Innovations in Magnetic Resonance for Early Detection of Cardiovascular Diseases. Current Pharmaceutical Design, 2015, 22, 77-89.	1.9	5
81	16-Channel Surface Coil for 13C-Hyperpolarized Spectroscopic Imaging of Cardiac Metabolism in Pig Heart. Journal of Medical and Biological Engineering, 2016, 36, 53-61.	1.8	5
82	Measured PET Data Characterization with the Negative Binomial Distribution Model. Journal of Medical and Biological Engineering, 2017, 37, 299-312.	1.8	5
83	CZT Detectors-Based SPECT Imaging: How Detector and Collimator Arrangement Can Determine the Overall Performance of the Tomograph. Electronics (Switzerland), 2021, 10, 2230.	3.1	5
84	A Compatible Electrocutaneous Display for functional Magnetic Resonance Imaging application. , 2006, 2006, 1021-4.		4
85	Developments in Imaging Technologies Related to Hypertensive Cardiovascular Diseases. Current Pharmaceutical Design, 2011, 17, 3081-3091.	1.9	4
86	Detection of 3D Cardiac metabolism after injection of hyperpolarized [1-13C]pyruvate. Journal of Cardiovascular Magnetic Resonance, 2011, 13, .	3.3	4
87	Structured errors in reconstruction methods for Non-Cartesian MR data. Computers in Biology and Medicine, 2013, 43, 2256-2262.	7.0	4
88	Simulation and comparison of coils for Hyperpolarized 13 C MRS cardiac metabolism studies in pigs. Measurement: Journal of the International Measurement Confederation, 2015, 60, 78-84.	5.0	4
89	Direct Parametric Maps Estimation from Dynamic PET Data: An Iterated Conditional Modes Approach. Journal of Healthcare Engineering, 2018, 2018, 1-14.	1.9	4
90	Cardiovascular Molecular Imaging: New Methodological Strategies. Current Pharmaceutical Design, 2013, 19, 2439-2446.	1.9	4

#	Article	IF	CITATIONS
91	Models and Methods in Cardiac Imaging for Metabolism Studies. Current Pharmaceutical Design, 2014, 20, 6171-6181.	1.9	4
92	New Imaging Frontiers in Cardiology: Fast and Quantitative Maps from Raw Data. Current Pharmaceutical Design, 2017, 23, 3268-3284.	1.9	4
93	A regression model of ultrasound reflectivity from normal myocardium. Medical Engineering and Physics, 1995, 17, 141-144.	1.7	3
94	Combining high-performance computing and networking for advanced 3-D cardiac imaging. IEEE Transactions on Information Technology in Biomedicine, 2000, 4, 58-67.	3.2	3
95	Regularization techniques on least squares nonâ€uniform fast Fourier transform. International Journal for Numerical Methods in Biomedical Engineering, 2013, 29, 561-573.	2.1	3
96	Negative binomial maximum likelihood expectation maximization (NB-MLEM) algorithm for reconstruction of pre-corrected PET data. Computers in Biology and Medicine, 2019, 115, 103481.	7.0	3
97	Probabilistic Graphical Models for Dynamic PET: A Novel Approach to Direct Parametric Map Estimation and Image Reconstruction. IEEE Transactions on Medical Imaging, 2020, 39, 152-160.	8.9	3
98	Can Imaging Techniques Identify Smoking-Related Cardiovascular Disease?. Current Pharmaceutical Design, 2010, 16, 2578-2585.	1.9	3
99	Dynamically variable electronic delays for ultrasound imaging. Journal of Biomedical Engineering, 1991, 13, 469-472.	0.7	2
100	A novel method for coil efficiency estimation: Validation with a 13C birdcage. Concepts in Magnetic Resonance Part B, 2012, 41B, 139-143.	0.7	2
101	Radio Frequency Coils for Hyperpolarized 13C Magnetic Resonance Experiments with a 3T MR Clinical Scanner: Experience from a Cardiovascular Lab. Electronics (Switzerland), 2021, 10, 366.	3.1	2
102	Fast and quantitative analysis of 4D cardiac images using a SMP architecture. Lecture Notes in Computer Science, 1998, , 447-451.	1.3	1
103	Signal-to-noise ratio improvement of cardiac magnetic resonance spectroscopy signals acquired by phased array coils: a simulation based approach. , 2008, , .		1
104	Comparison between volume and surface coils for pig cardiac metabolism studies with hyperpolarized 13C MRS. Journal of Cardiovascular Magnetic Resonance, 2011, 13, .	3.3	1
105	Segmental analysis of cardiac metabolism by hyperpolarized [1-13C] pyruvate: an in-vivo 3D MRI study in pigs. Journal of Cardiovascular Magnetic Resonance, 2012, 14, .	3.3	1
106	Filter design for phasedâ€array mr image reconstruction using super algorithm. Concepts in Magnetic Resonance Part B, 2012, 41B, 85-93.	0.7	1
107	A model-based method for myocardium flow estimation. Magnetic Resonance Materials in Physics, Biology, and Medicine, 2000, 11, 87-88.	2.0	0
108	Independent component analysis of fMRI data: a model based approach for artifacts separation. , 0, , .		0

#	Article	IF	CITATIONS
109	Physical principles of imaging with magnetic resonance. , 2005, , 1-29.		Ο
110	Automatic assessment of myocardial fibrosis by delayed enhanced magnetic resonance imaging. , 2008, ,		0
111	Reconstruction methods from hyperpolarized <sup>13</sup> C chemical shift imaging spiral 3D data: Comparison between direct summation and gridding method. , 2012, , .		0
112	The Influence of Noise in Dynamic PET Direct Reconstruction. IFMBE Proceedings, 2016, , 308-313.	0.3	0
113	A geographic network for MRI assessment of iron overload in thalassemia: the MIOT experience. , 2008, , .		0
114	Multislice Multiecho T2* Cardiovascular Magnetic Resonance Detects Heterogeneous Myocardial Iron Distribution in Thalassemia Patients. Blood, 2008, 112, 3877-3877.	1.4	0
115	Magnetic Resonance T2* Technique for Segmental and Global Quantification of Myocardial Iron : Multi-Centre Validation in the MIOT (Myocardial Iron Overload in Thalassemia) Network. Blood, 2008, 112, 5420-5420.	1.4	0
116	On-line 3D evaluation of left ventricular wall motion in magnetic resonance imaging. Technology and Health Care, 1998, 6, 151-7.	1.2	0